

Confirmation of simultaneous p and g mode excitation in HD 8801 and γ Peg from time-resolved multicolour photometry of six candidate "hybrid" pulsators

G. Handler

Institut für Astronomie, Universität Wien, Türkenschanzstrasse 17, A-1180 Wien, Austria

Accepted 2008 July 17. Received 2008 August 13; in original form 2008 September 10

ABSTRACT

We carried out a multi-colour time-series photometric study of six stars claimed as "hybrid" p and g mode pulsators in the literature. γ Peg was confirmed to show short-period oscillations of the β Cep type and simultaneous long-period pulsations typical of Slowly Pulsating B (SPB) stars. From the measured amplitude ratios in the Strömgren uvy passbands, the stronger of the two short period pulsation modes was identified as radial; the second is $\ell = 1$. Three of the four SPB-type modes are most likely $\ell = 1$ or 2. Comparison with theoretical model calculations suggests that γ Peg is either a $\sim 8.5 M_{\odot}$ radial fundamental mode pulsator or a $\sim 9.6 M_{\odot}$ first radial overtone pulsator. HD 8801 was corroborated as a "hybrid" δ Sct/ γ Dor star; four pulsation modes of the γ Dor type were detected, and two modes of the δ Sct type were confirmed. Two pulsational signals between the frequency domains of these two known classes of variables were confirmed and another was newly detected. These are either previously unknown types of pulsation, or do not originate from HD 8801. The O-type star HD 13745 showed small-amplitude slow variability on a time scale of 3.2 days. This object may be related to the suspected new type of supergiant SPB stars, but a rotational origin of its light variations cannot be ruled out at this point. 53 Psc is an SPB star for which two pulsation frequencies were determined and identified with low spherical degree. Small-amplitude variability was formally detected for 53 Ari but is suspected not to be intrinsic. The behaviour of ι Her is consistent with non-variability during our observations, and we could not confirm light variations of the comparison star 34 Psc previously suspected. The use of signal-to-noise criteria in the analysis of data sets with strong aliasing is critically discussed.

Key words: stars: variables: other – stars: variables: δ Scuti – stars: oscillations – stars: individual: γ Peg, 53 Psc, HD 8801, HD 13745, 53 Ari, ι Her, 34 Psc – stars: early-type – stars: – chemically peculiar

1 INTRODUCTION

Stars can self-excite observable pulsations if a driving mechanism operates in a resonant cavity in their interior or on their surface. This condition is fulfilled in certain parts of the HR diagram, causing the presence of different instability strips. A schematic representation of the domains of some confirmed classes of pulsating variable stars is given in Fig. 1.

The different types of pulsators have historically been classified phenomenologically, which has usually later turned out to have a physical reason. The individual classes can be separated in terms of types of excited pulsation modes, mass and evolutionary state. As can be seen in Fig. 1, the instability domains of some types of pulsators are not fully

distinct. Stars having two different sets of pulsational mode spectra excited simultaneously may therefore exist within overlapping instability strips. This is good news for asteroseismology – the study of stellar interiors based on modelling their pulsational spectra – as the information carried by both types of oscillations can be exploited.

In the past, there have been some reports of stars belonging to two different types of pulsating variables (Chapelier et al. 1987, Mathias & Waelkens 1995), but the first systematic survey for such "hybrid" pulsators was carried out by Handler & Shobbrook (2002). This search was successful in the discovery of both γ Dor-type g modes and δ Sct-type p modes in the star HD 209295 (CK Ind).

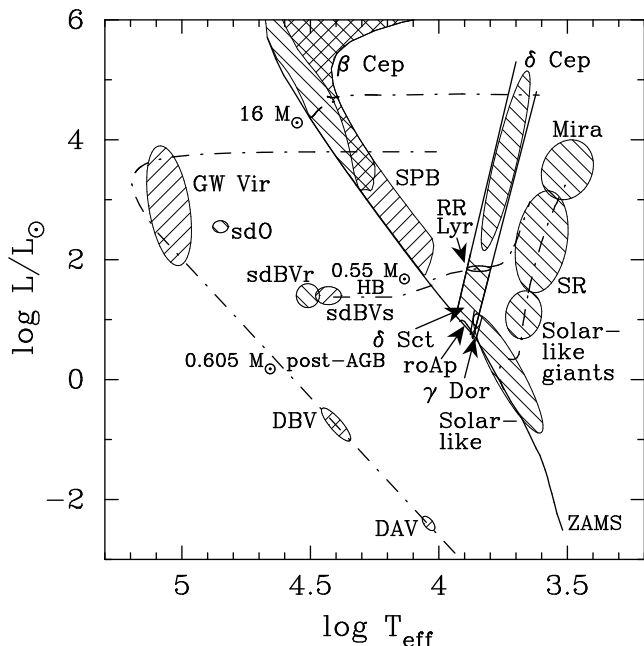


Figure 1. Theoretical HR diagram schematically showing the locations of different confirmed types of pulsating stars. Areas hatched from lower left to upper right depict domains of g-mode pulsators, areas hatched from lower right to upper left delineate domains of g-mode pulsators; overlapping areas may contain "hybrid" pulsators. Parts of model evolutionary tracks for main sequence, horizontal branch and post-AGB stars are shown as dashed-dotted lines for orientation. Adapted and updated from Christensen-Dalsgaard (2004).

However, Handler et al. (2002) showed that at least some of the g modes of CK Ind may have been excited through tidal effects from a close companion in an eccentric orbit. Following this work, Henry & Fekel (2005) discovered both γ Dor and δ Sct-type pulsations in the single Am star HD 8801, and the MOST satellite found two additional "hybrid" pulsators (HD 114839, King et al. 2006; BD+18 4914, Rowe et al. 2006) both of which are again Am stars. This is in itself interesting as Am stars have a lower incidence of pulsational variability than chemically "normal" A/F main sequence stars (e.g., see Kurtz 1989).

Among the B-type stars, "hybrid" SPB/ β Cep pulsations have been reported for several objects (e.g., see Jerzykiewicz et al. 2005, Handler et al. 2006, Chapellier et al. 2006, De Cat et al. 2007 [hereinafter DC07]). In addition, three subdwarf B stars were also discovered to show "hybrid" oscillations (Oreiro et al. 2005, Schuh et al. 2006, Lutz et al. 2009). The main physical difference between the B-type and A/F-type "hybrid" pulsators is that in the first group the same driving mechanism excites both types of oscillations, whereas in the δ Sct/ γ Dor stars two different driving mechanisms are at work.

A "hybrid" pulsator can therefore be characterized as a star that shows (at least) two distinct sets of different self-driven pulsational mode spectra, where the individual types of pulsations would belong to established classes of variable stars. As known examples, this could be a γ Dor star that shows simultaneous δ Sct pulsations or a β Cep star that also shows SPB-type pulsations etc.

The different types of oscillations in a "hybrid" pulsator would be well separated in frequency. Given the dispersion in the physical parameters within the known classes of pulsators, a better discriminant would be the pulsation constant $Q = P\sqrt{\bar{\rho}/\bar{\rho}_\odot}$, where P is the pulsation period and $\bar{\rho}$ is the mean stellar density. For instance, the most evolved δ Sct stars show periods that fall into the range of γ Dor oscillations, but the Q values of the two groups are cleanly separated (Handler & Shobbrook 2002). Consequently, mixed-mode pulsations by themselves are not "hybrid" pulsations because they occupy the same frequency domain as pure p modes.

The theoretical domains of B-type pulsators in the HR diagram are sensitive to the input element mixture and opacity tables (e.g., Miglio, Montalbán & Dupret 2007, Zdravkov & Pamyatnykh 2008), a natural consequence of the way their oscillations are driven. The driving is caused by the huge number of the transitions inside the thin structure of the electron shells in excited ions of the iron-group elements (Rogers & Iglesias 1994). Stankov & Handler (2005) noticed that the observed β Cep instability strip appears tilted with respect to the theoretically calculated boundaries, a problem nicely solved by models with revised solar abundances (Asplund et al. 2004) or OP opacities (e.g., Seaton 2005). As far as "hybrid" pulsators are concerned, the new input physics predicts a much larger overlap region between β Cep and SPB stars in the HR diagram, and the frequency ranges of the excited long and short period modes in "hybrid" B-type pulsators can pinpoint which opacities are to be favoured (Miglio et al. 2007, Zdravkov & Pamyatnykh 2008).

Pulsational driving of δ Sct stars is due to the κ mechanism operating in the HeII ionization zone (e.g., Chevalier 1971), whereas the driving mechanism for γ Dor stars is believed to be convective blocking (Guzik et al. 2000, Dupret et al. 2004). The latter mechanism is also expected to weaken or even exclude the driving of δ Sct-type pulsations. However, as the instability domains of these two types of variables overlap in the HR diagram (Handler 1999), "hybrid" δ Sct/ γ Dor pulsators have been searched for, with success.

Despite all the possibilities that "hybrid" pulsators offer for asteroseismology, the major observational problem that needs to be solved before arriving at a unique seismic model still remains the same - or is even more severe: a sufficiently large number of pulsation modes must be detected and identified - in *both* frequency domains.

An even more basic observational problem that needs to be solved when trying to discover "hybrid" pulsators is to prove that the variability, again in *both* frequency domains, is intrinsic and due to pulsation. For instance, some pulsating stars are the primary components of ellipsoidal variables (e.g., Chapellier et al. 2004). Finally, care must be taken that combination frequencies in frequency spectra are not mistaken for intrinsic pulsation modes.

Consequently, the best targets for asteroseismic studies of "hybrid" pulsators need to be firmly established before embarking on large-scale projects. To this end, we have selected six stars that have been claimed as "hybrid" pulsators in the abovementioned literature for such an exploratory study, comprising one main sequence A/F star and five O/B stars. All these objects are bright enough and were expected to have sufficiently large variability amplitudes to be observed with small ground-based telescopes.

1.1 Target stars

The bright star γ Peg (HD 886, B2IV) has been demonstrated to be a β Cep pulsator by Jerzykiewicz (1970). In the catalogue by Stankov & Handler (2005), it is the lowest-mass bona fide β Cep star and it is therefore close to the instability strip of the SPB stars (see Fig. 1). Chapellier et al. (2006) reported two periods in the β Cep range plus two periods in the SPB star range from several spectroscopic runs. Because neither of the published data sets on the star were extensive, these authors suggested the acquisition of new and accurate measurements. γ Peg was suggested as the primary component of a spectroscopic binary system. It is therefore possible that the slow variations might be due to imperfect removal of the orbital radial velocity variations. To confirm or reject the classification of γ Peg as a "hybrid" pulsator, a photometric study is ideal as no correction for orbital motion needs to be made; the light time effect is negligible.

HD 8801 (A7m) has been reported as a single Am star showing both δ Sct and γ Dor pulsations (Henry & Fekel 2005). These authors found two periods in the γ Dor domain, two in the δ Sct region, and two in between, with evidence for more. Interestingly, the pulsation constants of the two intermediate periods of HD 8801 are between the δ Sct and γ Dor domains. This raises the question whether or not HD 8801 has a companion, despite the lack of orbital radial velocity variations reported by Henry & Fekel (2005). If it has not, then what is the physical cause of these intermediate-period variations?

HD 13745 (V354 Per, O9.7II) and 53 Ari (HD 19374, B1.5V) have both been reported as "hybrid" β Cep/SPB stars by DC07 on the basis of photometric data. When examining the frequency analyses for these two stars (Figs. 21 and 22 of DC07), it becomes clear that these data suffer from severe 1 cd^{-1} aliasing and that the detection of the frequencies of the light variations were made at low signal-to-noise. This combination casts some doubt on the reality of the detections. We also note that while 53 Ari has a mass similar to γ Peg and is thus close to the β Cep instability strip and to the SPB domain, HD 13745 has been classified as an O-type star and may therefore be the most massive "hybrid" pulsator known to date.

ι Her (= HD 160762, B3IV) is the fifth "hybrid" pulsator candidate in this study, again possibly sharing the pulsational properties of the β Cep and SPB stars. It has been most extensively studied by Chapellier et al. (2000). These authors suggested that it is an SPB star that is located close to the edge of the β Cep instability strip and that the claimed short-period variations may be of transient nature. Therefore, some long-term monitoring was recommended. ι Her is also a known wide spectroscopic binary, with a secondary star considerably less massive than the primary (Abt & Levy 1978), and therefore unlikely to contribute to the system's recorded variability.

The claim of another "hybrid" pulsator, 53 Psc (= HD 3379, B2.5IV) has been refuted because the suggested short-period variations could not be confirmed (Le Contel et al. 2001, DC07). However, since 53 Psc is located only a few degrees away from the primary target γ Peg in the sky, we decided to include it in this study.

Table 1. Overview of the photometric observations. ΔT is the time span of the data set in days, T_{tot} is the total number of hours observed, N_{tot} is the number of nights observed, and N_{obs} is the number of data points obtained.

Star	ΔT	T_{tot}	N_{tot}	N_{obs}	Filters
γ Peg	69	284	48	884	uvy
53 Psc	69	281	48	861	uvy
HD 8801	69	272	48	737	vy
HD 13745	69	243	47	616	uvy
53 Ari	69	283	48	927	uvy
ι Her	78	137	46	631	uvy

2 OBSERVATIONS

We carried out differential time-series (u)vy photometry of the six stars mentioned above with the 0.75-m Automatic Photoelectric Telescope (APT) T6 at Fairborn Observatory in Arizona, between October 2007 and June 2008. An overview of the observations is given in Table 1.

As five targets are located at similar right ascension in the Northern sky, they can be observed simultaneously. We used one local comparison star for each target, four in total. The selection of comparison stars for differential photometry is crucial to the success of the project and must therefore be made carefully. In this work, the choice was based on two primary reasons: the comparison stars should be unlikely to show detectable variability, and they should, if possible, have been used in previous work so that we may be able to verify their photometric constancy within the accuracy of our measurements, and to compare our results with those in the literature.

The comparison star for γ Peg and 53 Psc was 34 Psc (HD 560, spectral type B9Vn), already used by Sareyan et al. (1979), and suspected to be a short-period variable by Jerzykiewicz & Sterken (1990). Because three stars were observed in this group, any possible variability in the differential light curves can be unambiguously ascribed to the star causing it. For HD 8801, we used HD 8671 (F7V) as local comparison. We expected that this rather cool star would not show photometrically detectable variability and it was used to examine our data for possible effects of differential colour extinction. The local comparison star for HD 13745 was HR 540 (HD 11408, A5m), as there was no suitable hotter star in this part of the sky. Kurtz (1977) tested HR 540 for variability and found it to be constant at the mmag level. The target 53 Ari was primarily compared to σ Ari (HD 17769, B7V), previously used as a comparison star by Sterken (1988) and not found variable. The remaining target ι Her was observed with the classical three-star method and with respect to 77 Her (HD 158414, A4V) and 30 Dra (HD 162579, A2V), previously observed by several authors (e.g., Chapellier et al. 2000, McMillan et al. 1976) and never found variable.

We decided to observe in several filters, because this helps in classifying the type of light variability (see Handler & Shobbrook 2002 for a discussion). In addition, if pulsation is detected, mode identifications can be obtained for variations with sufficient signal to noise. We employed the Strömgren vy filters for all targets for high precision and colour information plus the Strömgren u filter for possible

mode identification of the OB type target stars. The integration times were 40 s in each filter for each star to keep photon and scintillation noise below 1 mmag per measurement. A 10 s sky integration was obtained within each target/local comparison star group to take into account the dependence of sky brightness on position of the Moon and air mass.

Our observing strategy assured a minimum cadence of 25 minutes for consecutive target star measurements; if some targets were out of reach of the telescope, the cadence for the remainder was correspondingly higher. This enabled us to search for short periods because aliasing at the sampling frequency was smeared out considerably.

The data were reduced following standard photoelectric photometry schemes. First, the measurements were corrected for coincidence losses. Then, sky background was subtracted within each target/local comparison star group. Extinction coefficients were determined on a nightly basis from the measurements of all comparison stars via the Bouguer method (fitting a straight line to a magnitude vs. air mass plot). The same extinction correction was applied to each star. Finally, differential magnitudes were computed by interpolation, the timings were converted to Heliocentric Julian Date, and the data were subjected to analysis.

3 ANALYSIS AND RESULTS

The data were searched for periodicities using the program `Period04` (Lenz & Breger 2005). This software package uses single frequency Fourier and multifrequency nonlinear least squares fitting algorithms. The analysis was started by computing the spectral window function and the amplitude spectrum of the data, which were compared. If a signal was found to be present at a significant level and supposed intrinsic, it was fitted to the data, and its amplitude, frequency and phase were improved to obtain an optimal fit. Consequently, this variation was subtracted from the measurements (we call this procedure "prewhitening") and the residual amplitude spectrum was computed and examined. If more than one periodic signal was present, its parameters were optimized together with those of the ones previously detected. Once no significant variation was left in the residuals, the analysis was stopped. A signal was considered significant when it exceeded a S/N ratio of 4, following the empirical recommendation by Breger et al. (1993).

Before proceeding to the target stars, all possible differential light curves of the comparison stars with respect to each other were examined. No evidence for intrinsic variability of any of the chosen comparison stars was found within a level of ~ 2 mmag. Since the distances of the different target/local comparison star groups on the sky was of the order of tens of degrees, a $1/f$ component was present in most of the amplitude spectra of the magnitude differences between the comparison stars and some minor effects of differential (colour) extinction and/or variable sky transparency cannot be ruled out. However, as can be seen later, the differential light curves of the target stars had better quality due to the use of local comparison stars.

Turning to the targets, the frequency search was first performed for the light curves of each star in each filter individually. The solutions were compared. Despite some variation in the S/N in the different filters, we found ex-

Table 2. Multifrequency solution for our light curves of γ Peg. The formal errors on the amplitudes are ± 0.1 mmag in v and y and ± 0.2 mmag in u . The S/N ratio and formal frequency uncertainty are specified for the y filter data.

ID	Freq. (cd^{-1})	Amplitude			S/N
		u (mmag)	v (mmag)	y (mmag)	
f_1	6.5897 ± 0.0002	12.3	6.9	6.0	34.1
f_2	0.6343 ± 0.0005	3.4	2.1	2.0	10.5
f_3	0.6820 ± 0.0005	3.2	2.1	2.0	10.6
f_4	0.7407 ± 0.0007	2.3	1.7	1.5	7.8
f_5	6.0150 ± 0.0009	2.2	1.0	1.2	6.6
f_6	0.8841 ± 0.0011	1.9	1.2	1.0	5.2

cellent agreement between them. The light curves in the filter with the highest S/N data were chosen as reference for the acceptance of the reality of the signals. As the optimized frequency solutions varied from filter to filter within the errors, we adopted S/N-weighted averages as the final frequency values, fitted those to the light curves in the individual filters and re-determined the amplitudes, phases and S/N with these fixed frequencies. Formal error estimates for these parameters were determined with the formulae of Montgomery & O'Donoghue (1999); the real errors might be up to a factor of 2 higher (Handler et al. 2000, Jerzykiewicz et al. 2005).

3.1 γ Peg

The analysis of the amplitude spectrum of the y -filter data of γ Peg is shown in Fig. 2. As variations occur in two frequency domains, where the spectral window function of the single-site data is different, we have computed it in a non-standard way: it is the amplitude spectrum of two signals of 0.63 and 6.59 cd^{-1} with 5 mmag amplitude sampled in the same way as the original data (uppermost panel of Fig. 2). In this way, the aliases occurring at the reflection at frequency zero, which is important for the low-frequency domain, as well as the shape of the "pure" spectral window can both be displayed at once.

The amplitude spectrum of the data is dominated by the known β Cep pulsation of γ Peg. Prewhitening this signal leaves a small forest of low-frequency peaks that are all nicely resolved and unambiguously detected thanks to the high quality of our light curves (rms residuals of $4.0/3.2/2.7$ mmag per point in $u/v/y$).

We note that two frequencies separate in an amplitude spectrum if their difference is larger than the inverse of the length of the data set and that their amplitudes and phases can be determined free from systematic errors if their separation exceeds 1.5 times the inverse of the length of the data set (Loumos & Deeming 1978). In the present case $1.5/\Delta T = 0.022 \text{ cd}^{-1}$.

In the end, we could detect six independent signals in the light curves of γ Peg, four with frequencies around 0.7 cd^{-1} and two with frequencies around 6 cd^{-1} (Table 2). The amplitudes of all these signals increase with decreasing wavelength. No significant phase shifts between the different filters can be claimed for the individual oscillations.

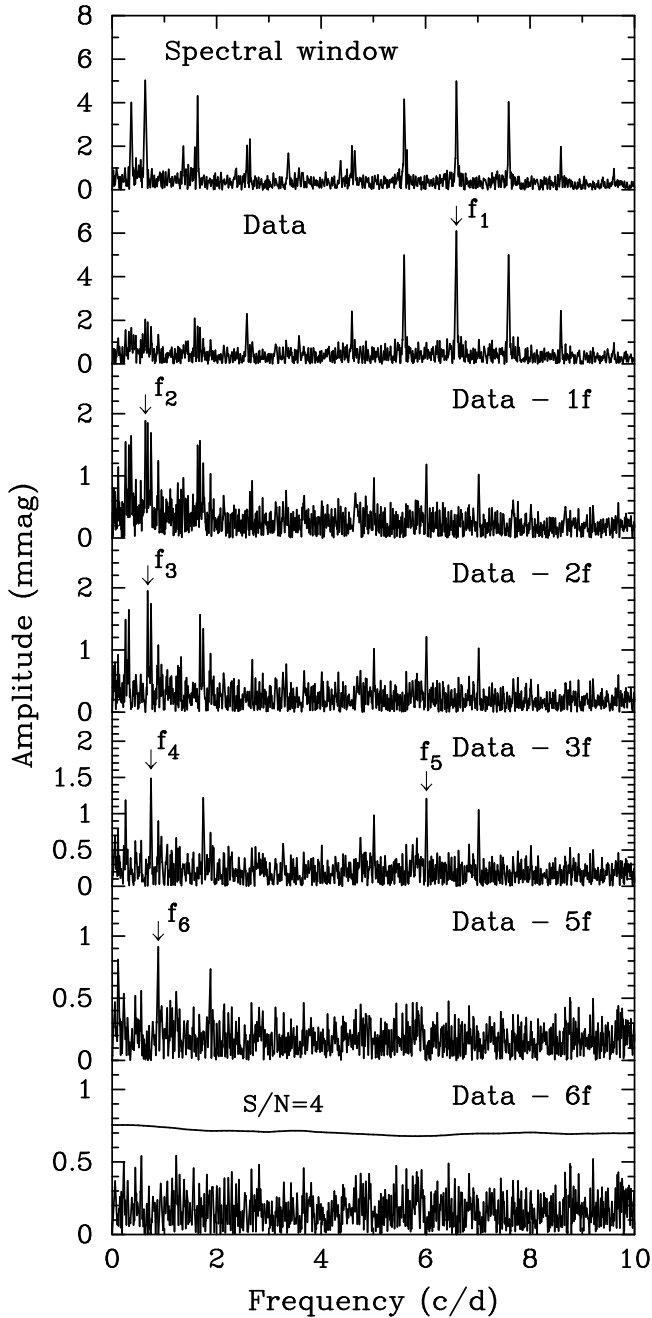


Figure 2. Spectral window and amplitude spectra of the y -filter light curves of γ Peg with consecutive stages of prewhitening. No variability was found outside the displayed frequency domain.

3.2 53 Psc

There is clear evidence for variability in the amplitude spectrum of the light curves of 53 Psc (second panel of Fig. 3). After prewhitening the strongest signal, a second variation with a frequency close to the first one becomes apparent. A two-frequency solution (Table 3) leaves no significant residual peak.

However, the residual 53 Psc amplitude spectrum contains a peak at 0.84 cd^{-1} at a S/N ratio of 3.7, which would form an equally spaced triplet with the two detected frequencies. Additional measurements are required to check

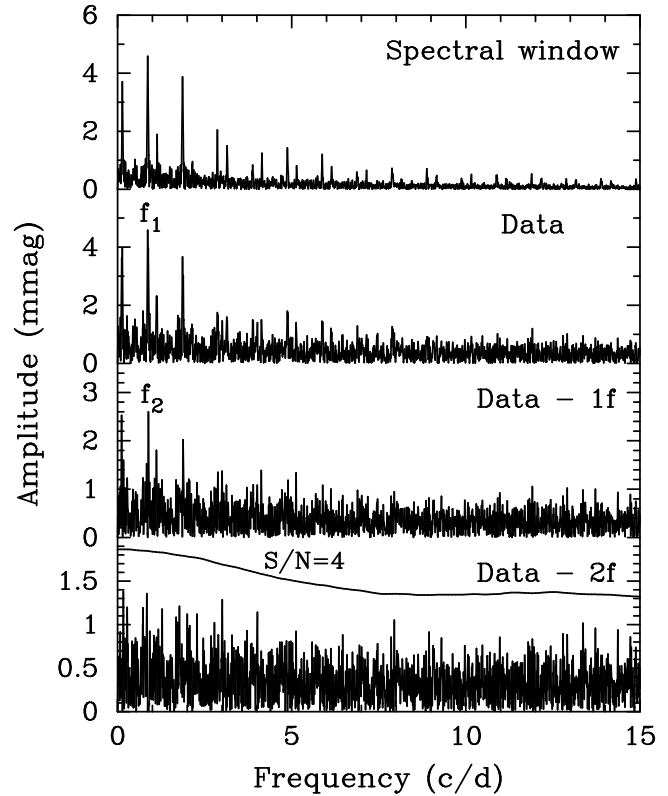


Figure 3. Spectral window (computed as the amplitude spectrum of a single signal with a frequency of 0.863 cd^{-1} and an amplitude of 4 mmag) and amplitude spectra of the u -filter light curves of 53 Psc with prewhitening of two closely-spaced frequencies. No variability was found outside the displayed frequency domain.

Table 3. Multifrequency solution for the light curves of 53 Psc. The formal errors on the amplitudes are ± 0.2 mmag for all three filters. The S/N ratio and formal frequency uncertainty are specified for the u filter data. The signals are in phase within the observational errors.

ID	Freq. (cd^{-1})	Amplitude			S/N
		u (mmag)	v (mmag)	y (mmag)	
f_1	0.8628 ± 0.0005	4.0	2.7	2.3	8.7
f_2	0.8833 ± 0.0007	2.7	1.7	1.2	6.0

its reality. The two detected signals have a separation of about 1.4 times the inverse length of the data set, which means they can be resolved, but our amplitude determinations may have some small systematic errors. Nevertheless, the observed trend that the smaller the effective wavelength of the used filter the larger the amplitudes become is undoubtedly real.

3.3 HD 8801

The amplitude spectrum of the measurements of HD 8801 immediately confirms that three distinct time scales are

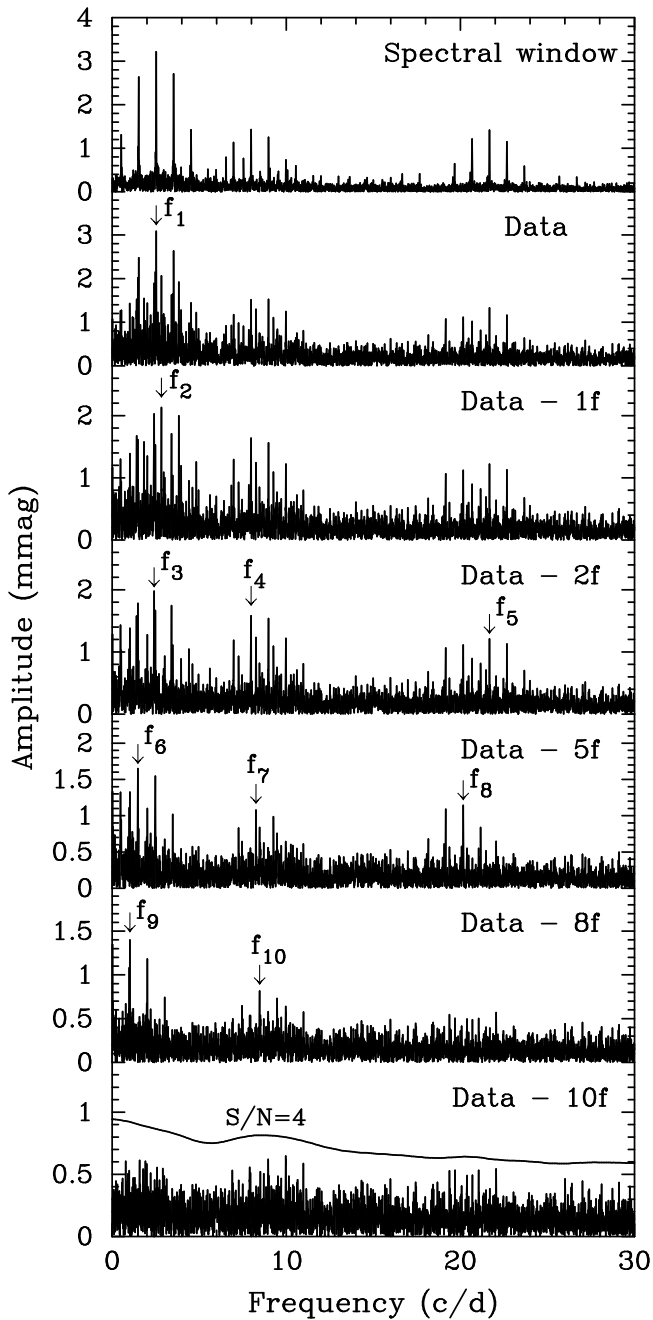


Figure 4. Spectral window (see text for details on its calculation) and amplitude spectra of the y -filter light curves of HD 8801 with consecutive stages of prewhitening. No variability was found outside the displayed frequency domain.

present in the star’s light variations. Therefore we have computed the spectral window of the data as the amplitude spectrum of an artificial light curve composed of three signals of 2.528, 7.976 and 21.669 cd^{-1} with y amplitudes of 3.2, 1.5 and 1.3 mmag, respectively (upper panel of Fig. 4). Comparing this spectral window with the amplitude spectrum of the real data immediately shows that the variability in all three frequency regions is multiperiodic.

Successive prewhitening reveals the presence of ten independent and well resolved frequencies in the light curves (Table 4); five between 1.0 and 2.8 cd^{-1} , three between 7.9

Table 4. Multifrequency solution for the light curves of HD 8801. The formal errors on the amplitudes are ± 0.2 mmag in v and ± 0.1 mmag in y . The S/N ratio and formal frequency uncertainty are specified for the y filter data. The phase differences of the individual signals between the two filters are consistent with zero within 1.1σ .

ID	Freq. (cd^{-1})	Amplitude		S/N
		v (mmag)	y (mmag)	
f_1	2.5277 ± 0.0003	4.4	3.2	14.6
f_2	2.8291 ± 0.0005	3.2	2.3	10.5
f_3	2.4057 ± 0.0006	3.0	2.0	9.1
f_4	7.9761 ± 0.0007	1.9	1.5	7.5
f_5	21.6692 ± 0.0008	2.0	1.3	8.4
f_6	1.4778 ± 0.0005	2.5	2.1	9.0
f_7	8.2607 ± 0.0010	1.5	1.1	5.3
f_8	20.1609 ± 0.0009	1.8	1.2	7.3
f_9	1.0178 ± 0.0008	2.1	1.4	6.3
f_{10}	8.4644 ± 0.0013	1.0	0.8	4.0

and 8.5 cd^{-1} and two between 20.1 and 21.7 cd^{-1} . The residual amplitude spectrum (lowest panel of Fig. 4) suggests that additional signals are likely present in the light variations. The v/y amplitude ratios of all signals listed in Table 4 (between 1.19 and 1.52) are indicative of pulsation (cf. theoretical predictions by, e.g., Garrido 2000).

None of the detected signals can be identified as having originated from combination frequencies, even taking into account possible aliasing ambiguities. The variation with frequency f_9 is difficult to be interpreted due to its proximity to 1 cycle per sidereal day. It is also possible that this signal is an alias from a long-term trend in the data, resulting in a peak at 0.018 cd^{-1} in the amplitude spectrum. However, the frequency $f_9 = 1.0178 \text{cd}^{-1}$ given in Table 4 results in a slightly better fit to the measurements.

3.4 HD 13745

This star shows some slow variability. Only a single frequency can be detected at a significant level (Fig. 5 and Table 5). After subtracting this signal, the highest peak in the residuals occurs at a frequency of 0.325 cd^{-1} in all three filters. While this may be taken as evidence that this signal is intrinsic, it does not reach a S/N ratio large enough for a significant detection. Still, there is a strong $1/f$ component in the residual amplitude spectrum that is not present in the residual periodograms of the other targets that were measured in the same nights. This implies that more intrinsic variability should be present in our measurements, but that we are unable to characterize it.

Interestingly, some signals around 9 cd^{-1} stand out of the noise in the residual amplitude spectrum (lower panel of Fig. 5); one even reaches formal significance. However, close inspection reveals that this peak coincides with the 9 cd^{-1} alias of the 0.325 cd^{-1} signal mentioned above, suggesting caution. Trial prewhitening of the signals near 9.3 cd^{-1} does not affect the ones near 0.3 cd^{-1} , but prewhitening the 0.325 cd^{-1} signal does make the 9.3 cd^{-1} peak disappear. We therefore conclude that these higher-frequency signals are spectral window effects

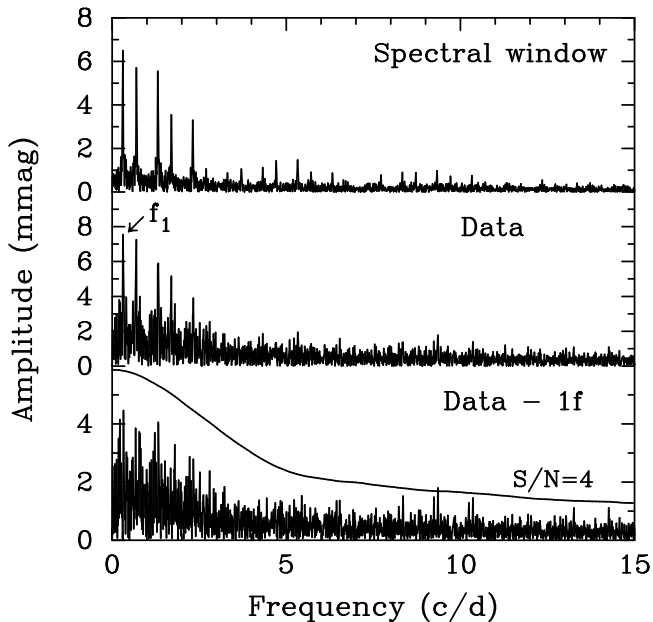


Figure 5. Spectral window (computed as the amplitude spectrum of a single signal with a frequency of 0.307cd^{-1} and an amplitude of 6 mmag) and amplitude spectra of the y -filter light curves of HD 13745 with prewhitening of one frequency. A formally significant peak near 9cd^{-1} remains, but is not judged intrinsic (see text). No variability was found outside the displayed frequency domain.

Table 5. Frequency solution for the light curves of HD 13745. The formal errors on the amplitudes are $\pm 0.4\text{ mmag}$ in the v and y filter, respectively, and $\pm 0.5\text{ mmag}$ in u . The S/N ratio and formal frequency uncertainty are specified for the y filter data. The variability is in phase in all three passbands within the observational errors.

ID	Freq. (cd^{-1})	Amplitude			S/N
		u (mmag)	v (mmag)	y (mmag)	
f_1	0.3071 ± 0.0005	8.0	7.2	7.5	5.3

that reach formal significance because of a lower influence of correlated noise in this frequency domain. The question remains why this occurred in the 9cd^{-1} region, and not in the frequency domain near 5cd^{-1} where aliasing is stronger in this data set.

3.5 53 Ari

The analysis of our measurements of 53 Ari is difficult (Fig. 6). There are two formally significant signals in the amplitude spectrum, but both are problematic. The strongest peak occurs close to 2 cycles per sidereal day and may therefore an effect of atmospheric extinction. The second signal that can be detected and is listed in Table 6 only reaches a formally significant level after prewhitening the dubious f_1 . Besides, its amplitude is very low in the u filter and it is buried in the noise there. We doubt that these two varia-

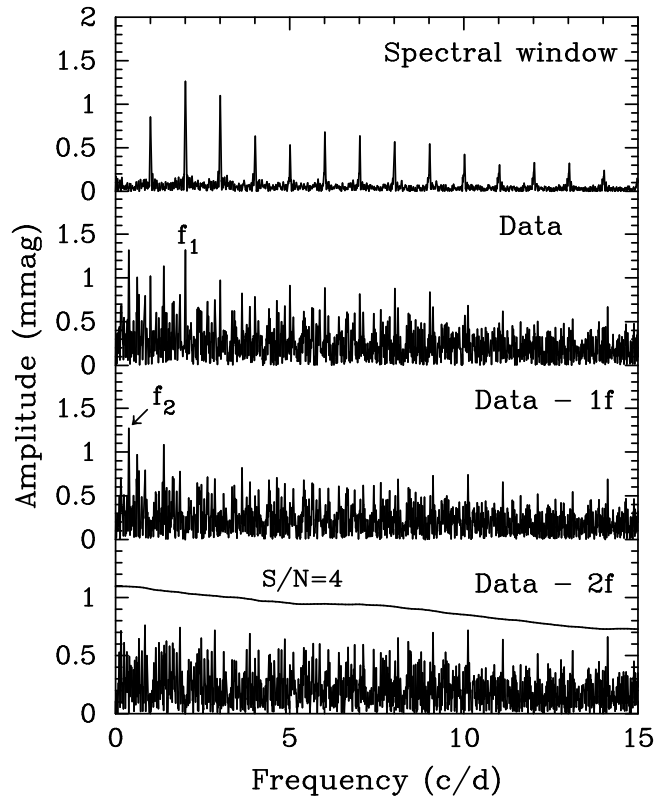


Figure 6. Spectral window (computed as the amplitude spectrum of a single signal with a frequency of 2.002cd^{-1} and an amplitude of 1.3 mmag) and amplitude spectra of the y -filter light curves of 53 Ari with prewhitening of two marginally significant frequencies. No variability was found outside the displayed frequency domain.

Table 6. Frequencies present in the light curves of 53 Ari. The formal errors on the amplitudes are $\pm 0.1\text{ mmag}$ in v and y and $\pm 0.2\text{ mmag}$ in u . The S/N ratio and formal frequency uncertainty are specified for the y filter data.

ID	Freq. (cd^{-1})	Amplitude			S/N
		u (mmag)	v (mmag)	y (mmag)	
f_1	2.0017 ± 0.0009	1.5	1.2	1.3	5.0
f_2	0.3796 ± 0.0009	0.8	1.0	1.3	4.7

tions are intrinsic to 53 Ari and only specify them in Table 6 for completeness and future reference.

3.6 ι Her

The amplitude spectrum of our measurements of ι Her contains no significant peak (Fig. 7). The noise in this amplitude spectrum has the same level and shape as that of the differential measurements of the comparison stars. The tallest peak seen in this y -filter amplitude spectrum is considerably less conspicuous than in v and completely absent in u . The behaviour of ι Her during our observations is therefore consistent with non-variability.

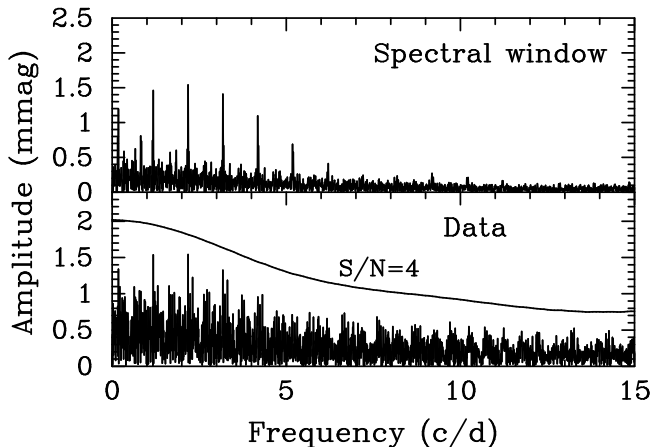


Figure 7. Spectral window (computed as the amplitude spectrum of a single signal with a frequency of 2.18 cd^{-1} and an amplitude of 1.5 mmag) and amplitude spectra of the y -filter light curves of ι Her. No variability was found.

4 DISCUSSION AND INTERPRETATION

To understand the nature of the variability of the target objects, knowledge about their positions in the HR diagram is required. These can be obtained by astrometric, photometric and spectroscopic means. We have collected the corresponding literature data and results for all our target stars.

Strömgren photometry indices are available for all targets from the online version of The General Catalogue of Photometric Data (GCPD; Mermilliod, Mermilliod & Hauck 1997). We used the program by Napiwotzki, Schönberner & Wenske (1993) that applies the T_{eff} calibration by Moon & Dworetzky (1985). Absolute magnitudes were determined from the new reduction of the Hipparcos parallaxes (van Leeuwen 2007), whenever significant. Otherwise, the M_v calibration by Balona & Shobbrook (1984) was used. With interstellar reddening determinations from Strömgren photometry and bolometric corrections tabulated by Flower (1996), we derived the stellar luminosities.

The GCPD also contains Geneva colour indices for all targets. We determined their effective temperatures and surface gravities from these data using the calibration by Künzli et al. (1997). DC07 used the same procedure for the three stars we have in common, the difference being that we used the values from the GCPD whereas they used the mean indices derived from their own Geneva measurements. The differences in the results are negligible.

The parameters derived from these basic resources can be supplemented by other work. Niemczura & Daszyńska-Daszkiewicz (2005) determined $\log T_{\text{eff}} = 4.342 \pm 0.011$ and $\log g = 3.82$ for γ Peg from low-resolution ultraviolet spectra. A NLTE model atmosphere analysis from optical spectra by Morel et al. (2006) resulted in $\log T_{\text{eff}} = 4.352 \pm 0.019$ and $\log g = 3.75 \pm 0.15$. These two spectroscopic results are in excellent agreement, and they also agree with the outcome of the calibrated photometry.

Concerning the Am star HD 8801, a spectral analysis of HD 8801 by R. Neuteufel (private communication) yields an effective temperature of $\sim 7500 \text{ K}$ and a surface gravity consistent with that of a ZAMS star. Spectroscopic

results are also available for ι Her. Niemczura (2003) derived $\log T_{\text{eff}} = 4.251 \pm 0.005$ and $\log g = 3.84$ from low-resolution ultraviolet spectra. Morossi et al. (2002) obtained $\log T_{\text{eff}} = 4.251 \pm 0.017$ and $\log g = 3.64 \pm 0.25$ from visual spectrophotometric measurements combined with ultraviolet spectra, and Lyubimkov et al. (2002) determined $\log T_{\text{eff}} = 4.230 \pm 0.006$ and $\log g = 3.77 \pm 0.12$ from a combination of several photometric and spectroscopic temperature and gravity indicators, in good agreement with previous literature values. For 53 Ari, Daszyńska-Daszkiewicz (private communication) determined $\log T_{\text{eff}} = 4.349$, $\log g = 3.55$ from IUE spectra, without available error estimates.

The remainder of the target stars have no spectroscopic temperature or surface gravity determinations. The only other constraint we found came from Walborn (2002), who derived the absolute magnitude of HD 13745 from its membership to the Per OB1 association with $M_v = -5.9 \text{ mag}$. No additional data are available for 53 Psc.

The results of the different determinations of the basic parameters of our targets quoted above are generally in good agreement, with one exception. For the most luminous program star, HD 13745, DC07 listed an effective temperature $\log T_{\text{eff}} = 4.550$ and $\log g = 4.03$ from Geneva photometry but cautioned that this was obtained by extrapolation from model atmosphere grids and may therefore be unreliable. However, these values yields a luminosity consistent with the estimates derived by us, although Strömgren photometry gives a considerably lower effective temperature that we prefer to use in this work, also because it is more consistent with the star's spectral luminosity classification. A spectroscopic temperature determination for HD 13745 is desirable.

The stellar parameters adopted for the present work, as derived from combining the information quoted above, are summarized in Table 7. The masses have been derived by placing the objects in a theoretical HR diagram and by comparing their positions with stellar models computed with the Warsaw-New Jersey stellar evolution code (e.g., see Pamyatnykh et al. (1998) for a description).

No current model input physics satisfy the conditions imposed by the oscillation behaviour of all pulsating stars and their positions in the HR diagram. Whereas OPAL opacities reproduce observed radial mode period ratios for δ Sct stars better than OP opacities (e.g., Lenz, Pamyatnykh & Breger 2007), the latter provide a better match to the excited frequency domains in β Cep pulsators (e.g., Miglio et al. 2007, Dziembowski & Pamyatnykh 2008). Consequently, we used OPAL opacities and the Grevesse & Noels (1993) element mixture to model the A/F star, but OP opacities and the Asplund et al. (2004) mixture for the OB stars. An overall metal abundance $Z = 0.02$ and a hydrogen abundance of $X = 0.7$ has been adopted for all models, and no convective core overshooting was used.

The locations of all target stars in the theoretical HR diagram are shown in Fig. 8, and are compared to observed (HD 8801) and theoretically predicted instability strips (OB star targets). All objects are inside the domains of "hybrid" pulsators, or no more than 2σ away from these regions, and they will be discussed individually in what follows.

Table 7. Basic parameters of the target stars derived from calibrated photometric systems, literature data and model evolutionary tracks. Error estimates have been conservatively adopted to include all possible sources of errors.

Star	$\log T_{\text{eff}}$	$\log L$	M/M_{\odot}
γ Peg	4.343 ± 0.019	3.77 ± 0.20	9.3 ± 1.0
53 Psc	4.251 ± 0.017	3.11 ± 0.15	6.2 ± 0.6
HD 8801	3.866 ± 0.009	0.77 ± 0.03	1.54 ± 0.03
HD 13745	4.397 ± 0.020	5.10 ± 0.25	22.5 ± 4.5
53 Ari	4.358 ± 0.017	3.47 ± 0.20	8.4 ± 0.9
ι Her	4.246 ± 0.017	3.27 ± 0.15	6.7 ± 0.6

4.1 γ Peg

Our study confirms beyond any doubt that γ Peg is a "hybrid" pulsator, as already suggested by Chapellier et al. (2006). In fact, the agreement of these spectroscopic results with our photometric measurements is surprisingly good, given the non-trivial analysis of the radial velocities. Both β Cep pulsation modes are present in the spectroscopy as well as the highest-frequency SPB oscillation. The three lowest-frequency SPB star pulsation modes are not resolved in the radial velocities.

We have attempted mode identifications of the pulsational signals detected. To this end, we followed the approach by Balona & Evers (1999) that uses theoretically calculated nonadiabatic parameters to determine the amplitude ratios between different wavebands that are the discriminator between the different modes of pulsation. We used the evolutionary models computed in the previous section and calculated theoretical uvy amplitudes for all pulsationally unstable modes along model sequences that spanned the physical parameter space of γ Peg as listed in Table 7. Only those modes whose frequencies were in the observed domain were considered. The resulting theoretical amplitudes in the three passbands were normalized to that in the u filter, and the average amplitude ratios and their rms errors were calculated. In this way we can also estimate the uncertainties involved in the calculation of theoretical results that need to be considered when being matched with the observations.

Using the parameters for γ Peg listed in Table 7, we arrived at the mode identification diagrams shown in Fig. 9. For modes f_1 and f_5 , a frequency domain between 5.8 and 6.8 cd^{-1} was scanned, for modes $f_2 - f_4$, we examined modes with frequencies of $0.62 - 0.76 \text{ cd}^{-1}$, and for mode f_6 the frequency range $0.86 - 0.91 \text{ cd}^{-1}$ was searched. We chose these narrow frequency domains because the pulsation constants change considerably over the observed g mode range, causing significant spread in the theoretical amplitude ratios (cf. Fig. 9).

We can interpret this diagram as follows: f_1 is certainly caused by a radial mode. The mode f_5 is suggested to be radial from Fig. 9, but the proximity of its frequency to f_1 ($f_5/f_1 = 0.913$) rules out such an identification. f_5 must therefore be nonradial, and due to its colour amplitudes would be most likely $\ell = 1$. Concerning the SPB star pulsation modes, f_2 , f_3 and f_4 are most likely $\ell = 1$ or 2, whereas no mode typing is possible for f_6 on the basis of the present data.

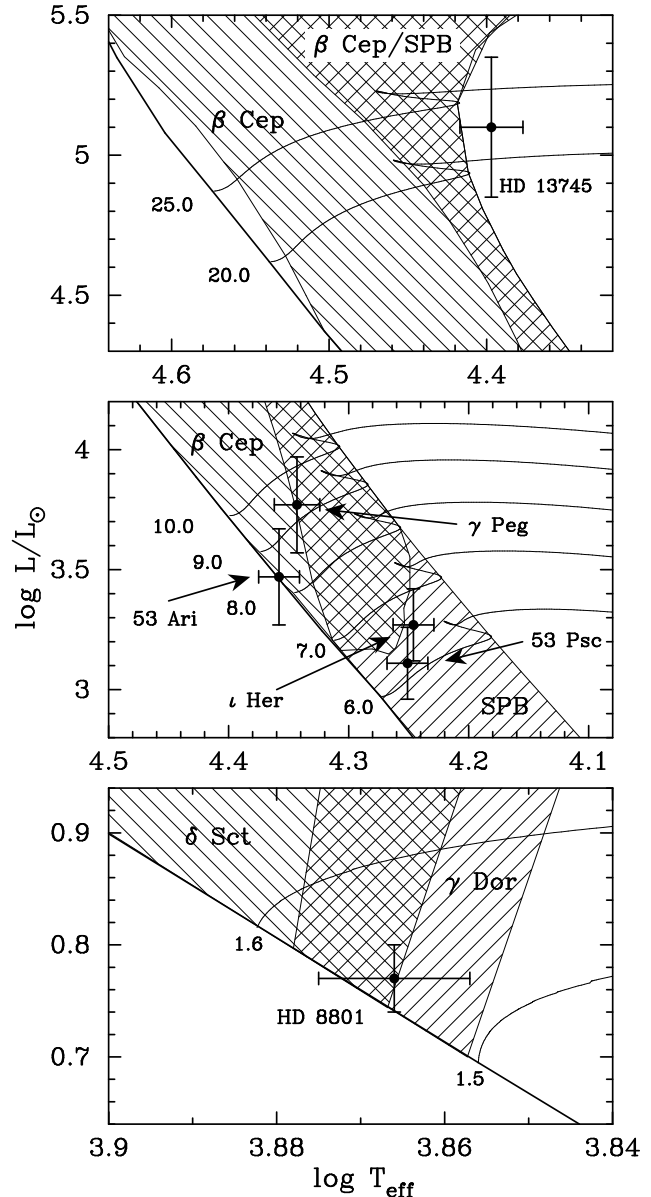


Figure 8. Theoretical HR diagram in the physical parameter domains of our target stars. The filled circles with the error bars denote the locations of the targets. Some evolutionary tracks labeled with their masses on the ZAMS are shown for comparison. Pulsational instability domains (Rodríguez & Breger 2001 for δ Sct stars, Handler & Shobbrook 2002 for γ Dor stars, Zdravkov & Pamyatnykh 2008 for β Cep and SPB stars) are indicated. Areas hatched from lower left to upper right are for g-mode pulsators, areas hatched from lower right to upper left for p-mode pulsators; regions of overlap consequently are cross-hatched.

Given the identification of f_1 as radial, consistent with previous literature results (Stamford & Watson 1977, Campos & Smith 1980), and given the near zero rotation of γ Peg (e.g., see Stankov & Handler 2005, Telting et al. 2006), we can try to identify f_5 , and to restrict the possible model parameter space for the star. We have a tight constraint on the mean stellar density for any given radial overtone corresponding to f_1 , and we have a constraint on the stellar mass (Table 7). Because β Cep stars are main sequence objects, their frequency spectra are sufficiently simple that one may

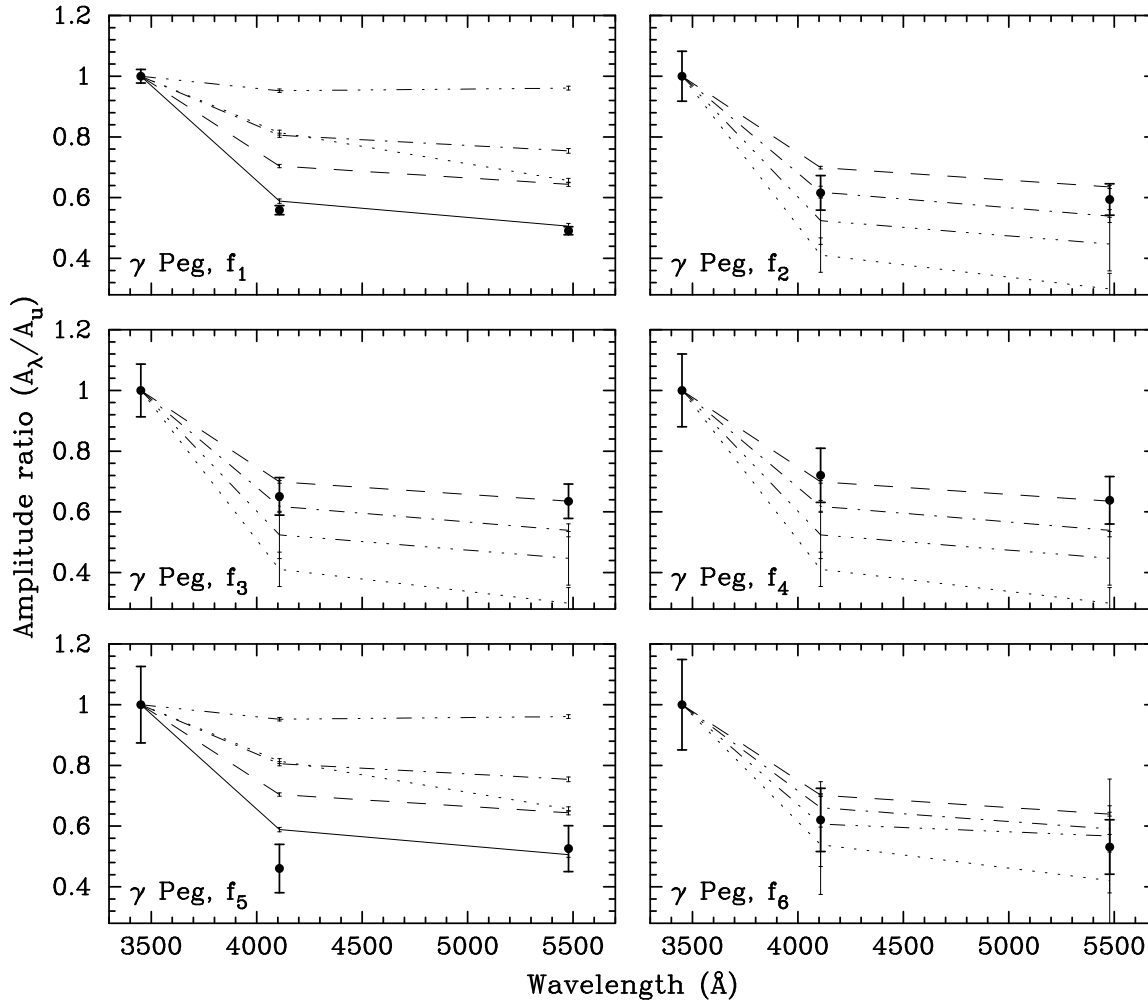


Figure 9. A comparison of the observed amplitudes of γ Peg in the different filters with theoretical predictions of pulsational wv amplitude ratios, normalized to unity at u . The filled circles with error bars are the observed amplitude ratios. The full lines are theoretical predictions for radial modes, the dashed lines for dipole modes, the dashed-dotted lines for quadrupole modes, the dotted lines for $\ell = 3$ modes, and the dashed-dot-dot-dotted lines are for $\ell = 4$. The thin error bars denote the uncertainties in the theoretical amplitude ratios.

hope that only a few modes have a frequency corresponding to f_5 in the possible parameter space.

We computed the corresponding models, again with the Warsaw-New Jersey stellar evolution and pulsation code. Because we only have two pulsation modes to fit, it is not possible to arrive at unique seismic models, but some constraints can be obtained.

For main sequence models with $9.3 \pm 1.0 M_{\odot}$, three radial modes can attain the observed frequency of $f_1 = 6.5897 \text{ cd}^{-1}$: the fundamental mode as well as the first and the second overtone. Assuming the radial mode to be the fundamental, we found that a model near $8.5 M_{\odot}$ has an $\ell = 1$, g_1 mode at the observed frequency of $f_5 = 6.015 \text{ cd}^{-1}$. If the radial mode was the first overtone, a $\sim 9.6 M_{\odot}$ model has an $\ell = 1$, p_1 mode at f_5 . Would the radial mode be the second overtone, an $\ell = 2$, p_2 mode would match f_5 for a mass of $\sim 9.4 M_{\odot}$. However, we can rule out such an identification from the colour amplitude ratios of f_5 in Fig. 9 that are inconsistent with such an $\ell = 2$ mode. Moreover, the corresponding model would have an effective temperature 2.2σ different from the value listed in Table 7. No further

model can reproduce the two β Cep frequencies within the assumptions made.

We are therefore left with two possibilities for the position of γ Peg in the HR diagram. Interestingly, the mode frequencies predicted by these two different models in the β Cep domain are in many cases similar. A distinction between these possibilities would therefore require the detection (and possibly identification) of several more of these pulsation modes that will, unfortunately, be of very low amplitude. In both possible models, the observed g modes would have radial overtones between $\sim 8 - 12$ for $\ell = 1$ and $\sim 14 - 21$ for $\ell = 2$, and thus are medium to high order g modes typical of SPB stars.

4.2 53 Psc

The observational history in terms of variability of this star has been nicely reviewed by DC07. In brief, β Cep-type variations were claimed by Sareyan et al. (1979), but later ascribed to originate from its comparison star 34 Psc (Jerzykiewicz & Sterken 1990). Le Contel et al. (2001) sug-

gested that multiperiodic SPB-type variations are present in their spectroscopic measurements, but these could at best only partly be confirmed by the photometric results of DC07.

We cannot confirm any of the literature results quoted above. Our data set exceeds the previous studies both quantitatively and qualitatively; we reached similar data quality as DC07, but have six times more measurements. One of the frequencies claimed by Le Contel et al. (2001) and DC07 is consistent with the 1 cd^{-1} alias of the strongest signal we found, as a re-analysis of the measurements of DC07 suggests.

Our frequency f_1 for 53 Psc is present in the amplitude spectrum of DC07's Geneva U data. Prewhitening it from the Geneva data causes disappearance of the strongest signal in this data set. We conclude that it was due to an unfortunate coincidence between low signal to noise and a poor spectral window. Because there is a time gap of several years between the measurements by DC07 and ours, combining the two data sets with a suitable choice of filters does not aid the analysis, that is, in any case, dominated by our measurements.

None of the other frequencies published by previous authors is present in our data either. By comparison of the three possible differential light curves between γ Peg, 53 Psc and their comparison star 34 Psc we can also exclude that 34 Psc showed short-period variations at the time scales reported earlier, within a limit of 0.5 mmag in the amplitude spectrum of the combined uvy data. The frequencies f_6 found for γ Peg and f_2 found for 53 Psc are the same within the observational errors. However, the analysis of the differential light curves of the comparison stars exclude the possibility that a variation on this time scale is due to 34 Psc.

53 Psc appears to be a normal SPB star. Telting et al. (2006) found high-degree line profile variations for this star, and DC07 interpreted the variability they found in the same way. We attempted mode identification of the two signals detected. Once more, we used the Warsaw-New Jersey stellar evolution and pulsation code to compute models in the parameter domain of interest (Table 7). We then calculated theoretical amplitude ratios of g modes with $1 \leq \ell \leq 4$ in a frequency range of $0.85 - 0.9 \text{ cd}^{-1}$ and compare them with the observations in Fig. 10.

The photometric amplitude ratios are consistent with pulsation with low spherical degree ℓ . We cannot rule out an $\ell = 1$ identification as DC07 did, although our error bars are smaller. This may be explicable with the fact that photometric mode identifications for B stars critically depend on ultraviolet amplitudes. Any systematic errors (as could for instance be caused by low S/N data) on these amplitudes have an adverse effect on the identifications. Finally, we remark that the high-degree line profile variability reported by Telting et al. (2006) is unlikely to correspond to the low-degree pulsations photometrically detected by us.

4.3 HD 8801

Given the limitations (single site observations) and differences (our time base is a factor of ~ 3.5 larger) in the data sets, our results agree well with those by Henry & Fekel (2005). In the γ Dor frequency domain, their strongest signal is a combination of the 1 cd^{-1} alias of our signal f_6 and

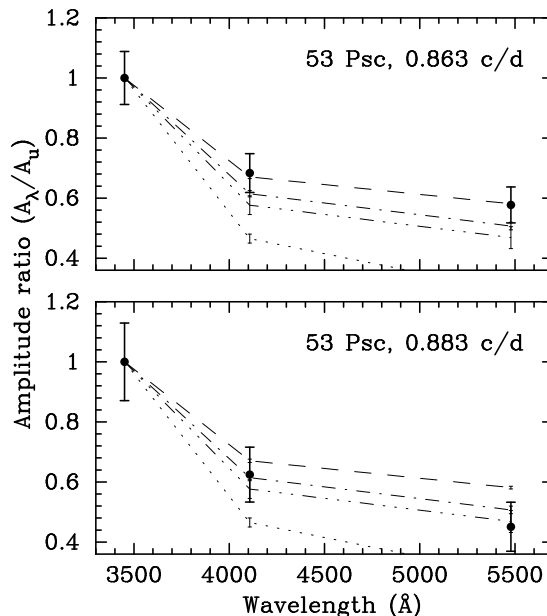


Figure 10. A comparison of the observed amplitudes of 53 Psc in the different filters with theoretical predictions of pulsational uvy amplitude ratios, normalized to unity at u . The filled circles with error bars are the observed amplitude ratios. The full lines are theoretical predictions for radial modes, the dashed lines for dipole modes, the dashed-dotted lines for quadrupole modes, the dotted lines for $\ell = 3$ modes, and the dashed-dot-dot-dotted lines are for $\ell = 4$. The thin error bars denote the uncertainties in the theoretical amplitude ratios. The variability is consistent with pulsation in $\ell = 1, 2$ or 4 modes.

our frequencies f_1 and f_3 that were unresolved in their data. The second strongest variation detected by Henry & Fekel (2005) in the γ Dor frequency range is consistent with our results within the errors. In the δ Sct domain, we find agreement with one frequency and the 1 cd^{-1} alias of the second, and in the intermediate frequency domain we again find consistency keeping in mind the different resolutions of the data sets.

We have attempted to identify at least the strongest modes with their spherical degree ℓ and constructed amplitude ratio/phase shift diagram as usually applied for δ Sct and γ Dor stars (e.g., see Watson 1988), for the Strömgren vy filters. We determined theoretical areas of interest in such a diagram following Balona & Evers (1999), only to find out that the large error bars on the observational amplitude ratios and phase shifts preclude any mode identification. Still, the observed v/y amplitude ratios strongly indicate that the variability of HD 8801 in all three frequency domains is due to pulsation, as already concluded by Henry & Fekel (2005).

To compute the pulsation constants Q of the individual oscillations, we derived a mean density of $\rho = 0.46 \pm 0.12 \rho_{\odot}$ from the values in Table 7. Therefore, the Q values have errors of $\sim 12\%$. For the modes with frequencies below 3 cd^{-1} , $0.24 < Q < 0.67$, consistent with high-order g -mode pulsation typical of γ Dor stars. For the two highest-frequency modes $0.031 < Q < 0.034$, consistent with low-order p -mode and mixed-mode pulsation typical of δ Sct stars.

For the three signals with intermediate frequencies, however, we calculate $0.080 < Q < 0.085$, corresponding to

low-order g modes ($k \sim 3$ for $\ell = 1$, $k \sim 5$ for $\ell = 2$). These Q values are *exactly* in between the domains of δ Sct and γ Dor stars (Handler & Shobbrook 2002), even taking into account the uncertainties determined above. This variability is therefore either a previously unknown type of stellar pulsation or it does not originate from HD 8801. The latter would require a so far undetected optical companion that is a δ Sct star near the TAMS, a rather unlikely scenario.

4.4 HD 13745

DC07 claimed the detection of "hybrid" β Cep/SPB pulsation in this star based on Geneva photometry. Our data set contains four times as many measurements at about the same data quality. We find no evidence for β Cep pulsation of HD 13745, and we cannot confirm any of the frequencies published by DC07. One of these frequencies ($f_3 = 0.6806 \text{ cd}^{-1}$) can be suspected to be an alias of the single significant variation in our data, but a re-analysis of the Geneva U measurements of DC07 does not support this idea. HD 13745 is therefore variable on time scales around 3.2 d, with no evidence for "hybrid" pulsations.

The parameters in Table 7 place the star somewhat beyond the TAMS in the HR diagram (cf. Fig. 8). We computed theoretical pulsational amplitude ratios for models between 17.5 to 27.5 M_{\odot} and compared them with the observed uvy amplitudes (Table 5). The results are consistent with pulsational variability. These models have modes excited at or near the observed frequency of light variation. These are high-order g modes (e.g., $k \sim 90$ for $\ell = 1$ or $k \sim 150$ for $\ell = 2$). However, since we only detected a single frequency of light variation with certainty, this still is no sufficient proof that the star is indeed a pulsator.

The published projected rotational velocity of HD 13745 is 260 kms^{-1} (Hill 1967). Table 7 implies a stellar radius of $19 \pm 7 R_{\odot}$. If the 0.3071 cd^{-1} variation we found was due to rotation, a rotational velocity of $295 \pm 110 \text{ kms}^{-1}$ would result. This is consistent with the measured $v \sin i$. We cannot exclude a rotational origin of the light variations at this point; the uvy amplitudes and phases of the detected signal do not provide additional clues. The excitation of r modes is another hypothesis that needs to be checked for HD 13745.

A conclusive interpretation of the variability of this star requires more observational data, or measurements from space. In addition, a more sophisticated approach to stellar modelling with respect to rotation (e.g., Dziembowski, Daszyńska-Daszkiewicz & Pamyatnykh 2007), is required as the time scales of the variability and rotation are of the same order. Both these efforts are far beyond the scope of the present work. The motivation for such studies may be drawn from the possible relation of HD 13745 to supergiants that are suspected SPB stars on the basis of investigations as suggested here (e.g., Saio et al. 2006).

4.5 53 Ari

The observational history of this object, classified as a runaway star by Blaauw (1956), in terms of variability, has been summarized by Sterken (1988). Photometric observations by this author did not reveal any light variations. Still, Gonzalez-Bedolla (1994) suggested the presence of short-period variations with a time scale between 0.5 and 1 hr.

"Hybrid" β Cep/SPB pulsation of 53 Ari was reported by DC07, based on 51 data points distributed over three years. Again, we cannot confirm this result, and in this case, we have collected 18 times more observations of comparable quality to DC07. Whereas we have formally detected two low-amplitude signals in our light curves, we are not convinced that these are intrinsic to the star (see Sect. 3.5). We therefore do not examine this eventual variability further.

However, the discrepancies between the results of DC07 and ours, for all three stars in common, require discussion. These authors reported the detection of more oscillations than we did, on the basis of often considerably smaller data sets. The difference lies in the use of signal-to-noise criteria for frequency detection. We have followed the suggestion by Breger et al. (1993) that signals with a S/N ratio exceeding 4 in an amplitude spectrum can be accepted as intrinsic, but have been cautious when approaching this limit. DC07 used a S/N limit of 3.6.

The S/N criterion by Breger et al. (1993) has been developed following an examination of several data sets, checking the reproducibility of the detection of the same frequencies in the same star. The test data were however taken at multiple sites and had fairly clean spectral windows. In most cases, the algorithms used for frequency analysis aim at a minimization of the residual scatter in the measurements. In a data set with limited temporal resolution and strong aliasing, such as single site observations, the average level of the noise peaks interfering with the spectral window function will therefore be reduced in the prewhitening process, and the residual noise level will be underestimated. Consequently, the significance of residual peaks in such an amplitude spectrum will be overestimated. None of the variations claimed by DC07 for the three stars we have in common exceeds an amplitude S/N ratio of 4 if Breger et al.'s (1993) criterion is applied in the originally proposed way. None of these variations is present in our measurements either, despite our noise levels being between about 1/2 to 1/4 of the ones reached by DC07.

We performed some tests as to whether or not the absence of the frequencies published by DC07 for the three stars in common can be explained by amplitude variations or beating or differences in detection threshold. None of these frequencies could be found down to a S/N ratio of only 2.5 (lower values were not considered) in our data. Merging the measurements by DC07 and/or the Hipparcos photometry of these stars with ours did not confirm any of these frequencies because our data sets dominate the combined analysis, no matter if using weights or not.

The width of the frequency interval in which the mean amplitude to determine the noise level at the frequency of interest is computed is a parameter to be carefully selected. It should be small enough to reflect any change in the local noise level depending on frequency, yet large enough to provide an accurate average: it must contain a sufficiently large number of independent frequencies. The present work used a 5 cd^{-1} interval. Finally, it must be kept in mind that the amplitude spectrum used to determine the noise level is oversampled. A frequency step of at least $1/10\Delta T$, where T is the length of the data set is required to take the sinc shape of individual the peaks properly into account. This work used a step of $1/20\Delta T$.

The discussion above illustrates why S/N criteria or

false alarm probabilities must be used with particular caution when examining data sets with complicated spectral window functions. We recall that Sect. 3.4 contains an example of a formally significant signal that was demonstrated to be spurious.

Pulsational mode identification from signals detected at low S/N in photometry of B-type stars is also problematic. The theoretical pulsation amplitudes of these stars increase towards the blue, as does the noise in (ground based) observational data. Consequently, a spurious signal can be easily misidentified as being due to a pulsation mode when examining photometric amplitude ratios, as the amplitude will tend to be higher in the blue and ultraviolet.

4.6 ι Her

The most extensive study of the variability of ι Her has been performed by Chapellier et al. (2000). These authors demonstrated the presence of low-amplitude SPB-type variability with a time scale of a few days both in photometry and in radial velocity, on top of orbital motion with a 113 d period. Short-period variability with a time scale of 3–4 hr was found in only one data set comprising seven consecutive nights of spectroscopy.

Our measurements could not confirm any of this variability. The absence of slow variations can be explained with the amplitude changes of ι Her reported by Chapellier et al. (2000). Turning to the short-term variations, our detection level for periods between 3–4 hr is around 1 mmag. The radial velocity amplitudes of the short-period signals found by Chapellier et al. (2000) were below 0.3 km s^{-1} , and quasi-simultaneous photometric observations did not show variability on these time scales either. Given the radial velocity to light amplitude ratios for main sequence early B stars (e.g., Cugier, Dziembowski & Pamyatnykh 1994), it is well possible that these possible variations have escaped detection in the aforementioned photometry and in our data set.

5 CONCLUSIONS

Asteroseismology of opacity-driven main sequence pulsators with their sparse mode spectra crucially depends on the correct determination of the intrinsic stellar pulsation frequencies and the correct identification of the oscillation modes causing them. Errors in this procedure will lead to incorrect seismic models, and incorrect conclusions about stellar physics will result.

This situation is to be avoided. Criteria that aid decisions which of the observed frequencies are acceptable as intrinsic have their limitations, and these have to be kept in mind. The final judgement of and responsibility for data interpretation are the scientist's. In times with ever improving quantities and quality of observational data it is important that the results not be overinterpreted, even if potentially exciting science provides temptation. Unfortunately, it usually takes more effort and resources to dispute a result from the literature safely than to make overoptimistic claims. Therefore, conservatism in data interpretation is prudent.

In the literature on some of the B star targets of the present work, transient short periods have been reported.

In most cases, these came from measurements poorly documented, and more extensive studies could never confirm them. Meanwhile, a wealth of information is present on B-type pulsators. Few of these stars show amplitude variability and if so, on time scales of many years (Jerzykiewicz & Pigulski 1999, Chapellier et al. 2000). Beating of several pulsation modes can sometimes generate single cycles of large-amplitude variability (which might just occasionally exceed the observational detection threshold; see also the discussion by Jerzykiewicz & Sterken 1990), but if the target is monitored intensively, at least some sign of them should be detectable in a periodogram. A sudden, single occurrence of short-period variability in a single, short data set of a well-monitored star otherwise quiescent on these time scales is therefore doubtful. It is suggested that the hypothesis of transient variability be set aside until convincingly proven.

The most interesting result from this study is the clear confirmation of the suspected "hybrid" β Cep/SPB pulsation of γ Peg, with four high-order *g* modes and two low-order *p* or mixed modes detected. The pulsation modes of the β Cep type were used to restrict the parameter space of possible models for the star in the HR diagram considerably: the presence of a radial mode immediately constrained the possible values for the mean density of the star. New measurements with a higher sensitivity, preferably from space, may make detailed asteroseismology of a "hybrid" pulsator possible for the first time. Consequently, the star has been put forward as a target for the MOST satellite (Walker et al. 2003).

We also confirmed that HD 8801 is a "hybrid" pulsator. In this object, even three distinct groups of oscillation mode frequencies were detected. Two of those correspond to pulsations of known types, i.e. HD 8801 is a δ Sct as well as a γ Dor star. The third range of excited modes is intermediate in frequency. If attributable to HD 8801, these represent a previously unobserved type of stellar oscillations whose excitation needs to be explained. An additional puzzle concerning "hybrid" δ Sct/ γ Dor stars is that all representatives known to date are Am stars (Matthews 2007), although the incidence of pulsation in Am stars is lower than in chemically normal A/F stars.

The only O star in our sample, HD 13745 showed slow, low-amplitude variability. Since this star may have left the main sequence, it could be related to the recently postulated supergiant SPB stars (Saio et al. 2006). This hypothesis requires confirmation. The most efficient strategy would be a high-resolution spectroscopic study, serving two purposes: to place the star in the HR diagram reliably, and to test whether or not the variability is indeed due to pulsation.

This study was unable to shed new light on the behaviour of ι Her. We failed to detect photometric variations during the observations, which might have been below our detection threshold. To understand the variability of this star, only a study involving simultaneous space photometry and high-resolution ground-based spectroscopy may suffice.

Concerning the two remaining target stars, 53 Psc was shown to be an SPB star. Two pulsation modes were detected, and some additional oscillations may be hidden in the observational noise. There is no evidence that this star also shows short-period oscillations reminiscent of a β Cep star. The same statement is true for 53 Ari that did not show convincing variability on longer time scales either.

ACKNOWLEDGEMENTS

This work has been supported by the Austrian Fonds zur Förderung der wissenschaftlichen Forschung under grant P20526-N16. The author is grateful to Peter De Cat for providing his observational data and for discussing the frequency analyses of DC07. Luis Balona, Wojtek Dziembowski and Alosza Pamyatnykh are thanked for permission to use their codes. Patrick Lenz provided some pulsation models during the earlier stages of this work. Vichi Antoci, Conny Aerts, Jadwiga Daszyńska-Daszkiewicz and Alosha Pamyatnykh supplied several helpful comments on the manuscript, and the constructive remarks of the anonymous referee made this paper more complete.

This paper has been typeset from a \TeX / \LaTeX file prepared by the author.

REFERENCES

- Abt H. A., Levy S. G., 1978, *ApJS* 36, 241
 Asplund M., Grevesse N., Sauval A. J., Allende Prieto C., Kiselman D., 2004, *A&A* 417, 751
 Balona L. A., Shobbrook R. R., 1984, *MNRAS* 211, 375
 Balona L. A., Evers E. A., 1999, *MNRAS* 302, 349
 Blaauw A., 1956, *ApJ* 123, 408
 Breger M., et al., 1993, *A&A* 271, 482
 Campos A. J., Smith M. A., 1980, *ApJ* 238, 250
 Chapellier E., et al., 1987, *A&A* 176, 255
 Chapellier E., Mathias P., Le Contel J.-M., Garrido R., Le Contel D., Valtier J.-C., 2000, *A&A* 362, 189
 Chapellier E., et al., 2004, *A&A* 426, 247
 Chapellier E., Le Contel D., Le Contel J.-M., Mathias P., Valtier J.-C., 2006, *A&A* 448, 697
 Chevalier C., 1971, *A&A* 14, 24
 Christensen-Dalsgaard, J., 2004, in *Helio- and Asteroseismology: Towards a Golden Future*, ed. D. Danesy, ESA-SP 559, p. 1
 Cugier H., Dziembowski W. A., Pamyatnykh A. A., 1994, *A&A* 291, 143
 De Cat P., et al., 2007, *A&A* 463, 243 (DC07)
 Dupret M. A., Grigahcène A., Garrido R., Gabriel M., Scuflaire R., 2004, *A&A* 414, L17
 Dziembowski W. A., Daszyńska-Daszkiewicz J., Pamyatnykh A. A., 2007, *MNRAS* 374, 248
 Dziembowski W. A., Pamyatnykh A. A., 2008, *MNRAS* 385, 2061
 Flower P. J., 1996, *ApJ* 469, 355
 Garrido R., 2000, in *Delta Scuti and Related Stars*, eds. M. Breger and M. Montgomery, ASP Conf. Ser. 210, p. 67
 Gonzalez Bedolla S., 1994, in Balona L. A., Henrichs H. F., Le Contel J.-L. (eds) *Pulsation, Rotation and Mass Loss in Early Type Stars*, Proc. IAU Symp. 162, Kluwer Academic Press, Dordrecht, Holland, p. 31
 Grevesse N., Noels A., 1993, in Prantzos N., Vangioni-Flam E. and Casse M., eds, *Origin and Evolution of the Elements*, Cambridge University Press, p. 15
 Guzik J. A., Kaye A. B., Bradley P. A., Cox A. N., Neuforge C., 2000, *ApJ* 542, L57
 Handler G., 1999, *MNRAS* 309, L19
 Handler G., Shobbrook R. R., 2002, *MNRAS* 333, 251
 Handler G., et al., 2000, *MNRAS* 318, 511
 Handler G., et al., 2002, *MNRAS* 333, 262
 Handler G., et al., 2006, *MNRAS* 365, 327
 Henry G. W., Fekel F. C., 2005, *AJ* 129, 2026
 Hill G., 1967, *ApJS* 14, 263
 Jerzykiewicz M., 1970, *Acta Astron.* 20, 93
 Jerzykiewicz M., Sterken C., 1990, *A&A* 227, 77
 Jerzykiewicz M., Pigulski A., 1999, *MNRAS* 310, 804
 Jerzykiewicz M., Handler G., Shobbrook R. R., Pigulski A., Medupe R., Mokgwetsi T., Tlhagwane P., Rodríguez E. 2005, *MNRAS* 360, 619
 King H., et al., 2006, *CoAst* 148, 28
 Künzli M., North P., Kurucz R. L., Nicolet B., 1997, *A&AS* 122, 51
 Kurtz D. W., 1977, *PASP* 89, 939
 Kurtz D. W., 1989, *MNRAS* 238, 1077
 Le Contel J.-M., Mathias P., Chapellier E., Valtier J.-C., 2001, *A&A* 380, 277
 Lenz P., Breger M., 2005, *CoAst* 146, 53
 Lenz P., Pamyatnykh A. A., Breger M., 2007, in *Unsolved Problems in Stellar Physics: A Conference in Honor of Douglas Gough*, AIP Conf. Proc. Vol. 948, p. 201
 Loumos G. L., Deeming T. J., 1978, *Ap&SS* 56, 285
 Lutz R., Schuh S., Silvotti R., Bernabei S., Dreizler S., Stahn T., Huegelmeier S. D., 2009, *A&A*, in press, arXiv:0901.4523
 Lyubimkov, L. S., Rachkovskaya T. M., Rostopchin S. I., Lambert D. L., 2002, *MNRAS* 333, 9
 Mathias P., Waelkens C., 1995, *A&A* 300, 200
 Matthews J. M., 2007, *CoAst* 150, 333
 McMillan R. S., Breger M., Ferland G. J., Loumos G. L., 1976, *PASP* 88, 495
 Mermilliod J.-C., Mermilliod M., Hauck B., 1997, *A&AS* 124, 349
 Miglio A., Montalbán J., Dupret M.-A., 2007, *MNRAS* 375, L21
 Moon T. T., Dworetzky M. M., 1985, *MNRAS* 217, 305
 Morel T., Butler K., Aerts C., Neiner C., Briquet M., 2006, *A&A* 457, 651
 Morossi C., Di Marcantonio P., Franchini M., Malagnini M. L., Chavez M., 2002, *ApJ* 577, 377
 Napiwotzki R., Schönberner D., Wenske V., 1993, *A&A* 268, 653
 Niemczura E., 2003, *A&A* 404, 689
 Niemczura E., Daszyńska-Daszkiewicz J., 2005, *A&A* 433, 659
 Oreiro R., Perez Hernandez F., Ulla A., Garrido R., Østensen R., MacDonald J., 2005, *A&A* 438, 257
 Pamyatnykh A. A., Dziembowski W. A., Handler G., Pikall H., 1998, *A&A* 333, 141
 Pamyatnykh A. A., Handler G., Dziembowski W. A., 2004, *MNRAS* 350, 1022
 Rodríguez E., Breger M., 2001, *A&A* 366, 178
 Rogers F. J., Iglesias C. A., 1994, *Science* 263, 50
 Rowe J. F., et al., 2006, *CoAst* 148, 34
 Saio H., et al., 2006, *ApJ* 650, 1111
 Sareyan J.-P., Le Contel J.-M., Ducatel D., Valtier J.-C., 1979, *A&A* 72, 313
 Schuh S., Huber J., Dreizler S., Heber U., O'Toole S. J., Green E. M., Fontaine G., 2006, *A&A* 445, L31
 Seaton M. J., 2005, *MNRAS* 362, L1
 Stamford P. A., Watson R. D., 1977, *MNRAS* 180, 551
 Stankov A., Handler G., 2005, *ApJS* 158, 193
 Sterken C., 1988, *A&A* 189, 81
 Teltel J. H., Schrijvers C., Ilyin I. V., Uytterhoeven K., De Ridder J., Aerts C., Henrichs H. F., 2006, *A&A* 452, 945
 van Leeuwen F., 2007, *A&A* 474, 653
 Walborn N. R., 2002, *AJ* 124, 507
 Walker G., et al., 2003, *PASP* 115, 1023
 Watson, R. D., 1988, *Ap&SS* 140, 255
 Zdravkov T., Pamyatnykh A. A., 2008, *JPhCS* 118, 012079